Climatological Analysis of Atmospheric Rivers in the Eastern Pacific: A Comparative Study

Deveshi Buch

Vista del Lago High School, Folsom, CA

INTRODUCTION

Atmospheric Rivers: Characteristics & Impacts

Atmospheric Rivers (ARs) are responsible for >90% of poleward transport of water vapor across the mid-latitudes [Zhu and Newell 1998]. Typically, an AR is associated with the warm conveyor belt (WCB) of an extratropical cyclone. An AR has the following properties [Ralph et al. 2004, 2005]: (1) a narrow band of high specific humidity, (2) high wind speeds in a pre-cold-frontal low level jet, and (3) low-level instability. ARs are long, narrow regions with Integrated Water Vapor (IWV) ≥20 kgm^{-2} (mm), and Integrated Vapor Transport (IVT) ≥250 $kgm^{-1}s^{-1}$ [Ralph et al. 2004; Rutz et al. 2014]. AR events are responsible for bringing significant precipitation to Western North America and replenishing water resources, but they are also notorious for catastrophic floods. California's water supply depends greatly upon ARs, which provide 25-50% of a water-year's precipitation [Dettinger et al. 2011]. Because of the importance of ARs for water resource management, it is necessary to analyze the characteristics of different types of ARs over a relatively long period of time.

Fig. 1

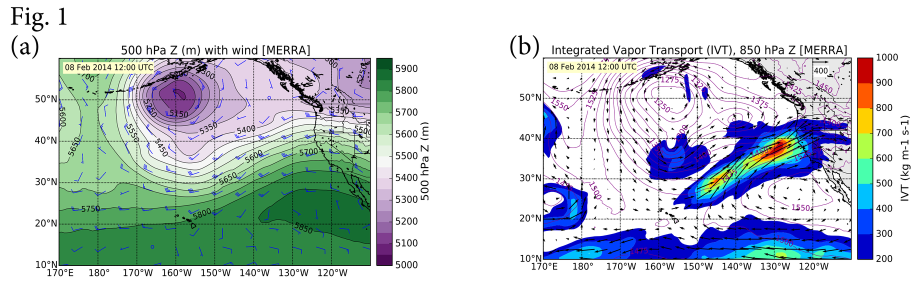

A previous study focused on characterizing the AR event in early February 2014 (Fig. 1) and considered this event in a climatological context of recorded ARs occurring in the month of February over the 20-year period from 1996-2015.

OBJECTIVES

(1) Extend the previous study with a climatological characterization for the month of November over the same twenty-year period, 1996-2015. Compare and contrast with the February AR climatology.

(2) Expand the analysis using multiple landfall points along the California coast.

(3) Explore the overarching challenge of the identification and classification of AR events using machine learning techniques.

MATERIALS & METHODS

Data is obtained from European Centre for Medium-Range Weather Forecasts (ECMWF) ERA-Interim reanalysis datasets for February and November from 1996-2015 at a resolution of 3/4 × 3/4 deg. Dates of observed landfalling ARs for WY 1998-2008 impacting CA (32.5°N-41.0°N) are from SSM/I ascending and descending passes [Dettinger et al. 2011; Neiman et al. 2008 (Met.)]. AR dates for the remaining years are calculated here based on ECMWF reanalysis with the constraint of IWV ≥20 mm and IVT ≥250 $kgm^{-1}s^{-1}$ for observations 12 hrs apart. These calculations are performed for a single point (38.25°N,123.00°W) and for five points along the California coast (33.00-40.50°N,117.75-124.50°W); for the latter, the maximum IWV and IVT values at these points are calculated. Data processing, analysis, and plot generation are performed by custom Python code using NumPy and the NetCDF4, Matplotlib, and Basemap modules. Panoply is used for brief data visualization.

Processing Flow

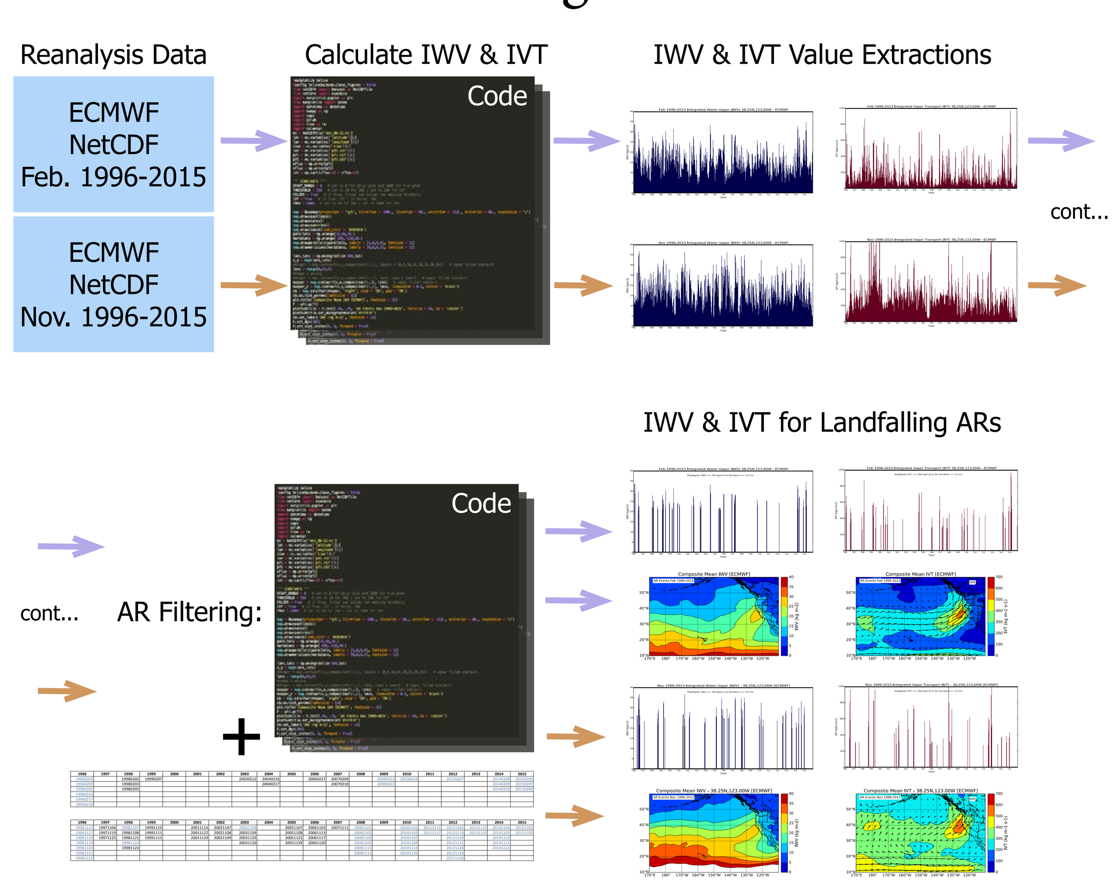

IWV (Integrated Water Vapor) is mathematically defined as:

$$\mathrm{IWV} = \frac{1}{g}\int q\,\mathrm{d}p$$

where g is the gravitational acceleration in ms^{-2}, q is the specific humidity in $kgkg^{-1}$, and $\mathrm{d}p$ in Pa is the pressure delta between adjacent pressure levels [Rutz et al. 2014].

IVT is vertically integrated horizontal water vapor transport [Zhu and Newell 1998; Neiman et al. 2008 (Dia.)] and is mathematically defined as:

$$\mathrm{IVT} = \sqrt{\left(\frac{1}{g}\int qu\,\mathrm{d}p\right)^2 + \left(\frac{1}{g}\int qv\,\mathrm{d}p\right)^2}$$

where the additional terms u and v are the zonal and meridional winds in ms^{-1}.

RESULTS

Climatology of AR Events

Fig. 2

(a) FEBRUARY

1996	1997	1998	1999	2000	2001	2002	2003	2004	2005	2006	2007	2008	2009	2010	2011	2012	2013	2014	2015
19960203		19980202	19990207				20030212	20040216		20060227	20070209		20090222	20100224		20120207		20140208	20150206
19960204		19980203						20040217			20070210		20090223					20140209	20150207
19960205		19980205																20140210	20150208
19960216																			
19960217																			
19960219																			

(b) NOVEMBER

1996	1997	1998	1999	2000	2001	2002	2003	2004	2005	2006	2007	2008	2009	2010	2011	2012	2013	2014	2015
19961113	19971106	19981107	19991110		20011116	20021107	20031108		20051107	20061103	20071111	20081101		20101101	20111111	20121101	20131119	20141104	20151101
19961117	19971119	19981108	19991111		20011122	20021108	20031109		20051108	20061113		20081102		20101102	20111112	20121119	20131120	20141105	20151102
19961118	19971125	19981121	19991115		20011129	20021109	20031129		20051125	20061117		20081103		20101107		20121120		20141113	
19961119		19981122					20031130		20051129	20061120		20081106		20101108		20121121		20141121	
19961120		19981123										20081111		20101114		20121128		20141122	
19961121												20081112		20101120		20121129			
19961122																20121130			

Fig. 2 (a) and (b) show, respectively, the recorded AR events for February and November from 1996-2015. Dates of observed landfalling ARs for WY 1998-2008 impacting CA (32.5°N-41.0°N) are from SSM/I ascending and descending passes [Dettinger et al. 2011; Neiman et al. 2008 (Met.)]. AR dates for the remaining years are calculated here based on ECMWF reanalysis with the constraint of IWV ≥20 mm and IVT ≥250 $kgm^{-1}s^{-1}$ for observations 12 hrs apart. All dates shown in blue are from this study. It can be observed that there are many more AR events in November (43) across the twenty-year period than in February (15).

AR Events: February & November, 1996-2015 (Single Location)

Fig. 3

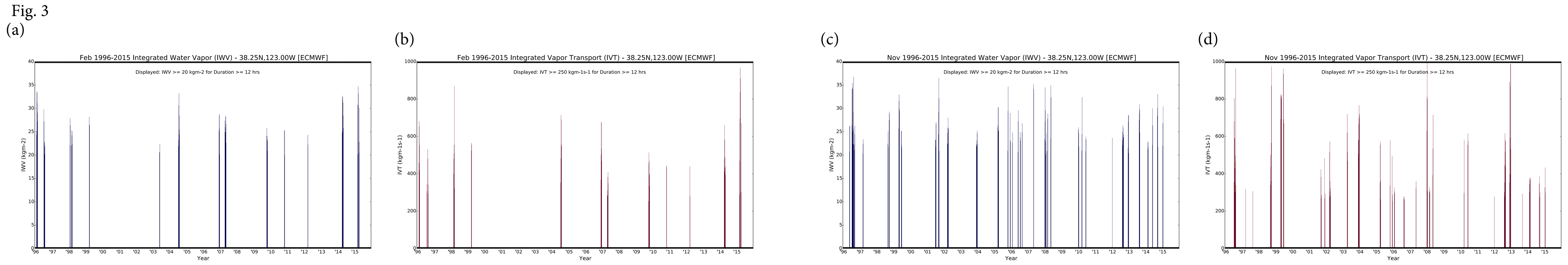

The 20-year data for IWV and IVT in Fig. 3 (a) and (b) are for Feb. 1996-2015, at 6 hr intervals, for 38.3°N,123.0°W. An algorithm was developed in Python to filter this raw data to meet a threshold of ≥20 kgm-2 (IWV) and ≥250 $kgm^{-1}s^{-1}$ (IVT), to expose those values that likely represent AR events. The AR events from Fig. 2 appear to be present in the filtered data. Note that values of IWV/IVT that meet criteria do not solely establish the presence of an AR. Data in Fig. 3 are for a location in proximity to the Bodega Bay Atmospheric River Observatory in California, whereas the AR events recorded in Fig. 2 correspond to 32.5°N-41.0°N. Also, note the absence of an IVT peak for Feb. 2003 in Fig. 3 (b). Additionally, several AR events that are present in (c) are not present in (d), such as the first event of November 1996 and the event of November 2003. Furthermore, the relative number of AR events in November is far greater than the number of events in February, over the period studied.

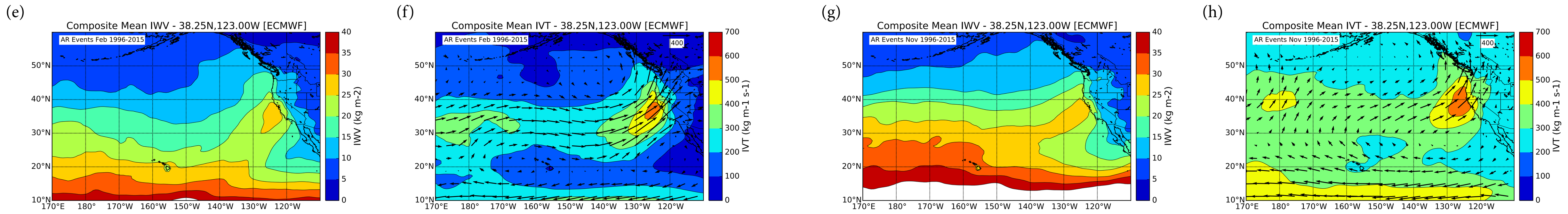

Fig. 3 (e) and (f) show the composite mean IWV and IVT values for February ARs in the 1996-2015 period; (g) and (h) show these for November. At the core of both composite ARs, peak IWV of 25-30 mm and peak IVT of 500-600 $kgm^{-1}s^{-1}$ are observed. However, (g) shows the IWV for the November events extending beyond its core to the tropical water vapor reservoir, which appears at a higher latitude compared to (e). Furthermore, the IVT values for the November composite in (h) are higher than those of February in (f) but form a less-pronounced composite AR. It can be observed that the February composite AR in (e) tends to have a more meridional form compared to the November composite AR in (g), possibly linked with the apparent poleward extension of moisture from the tropical water vapor reservoir.

AR Events: February & November, 1996-2015 (Multiple Locations)

Fig. 4

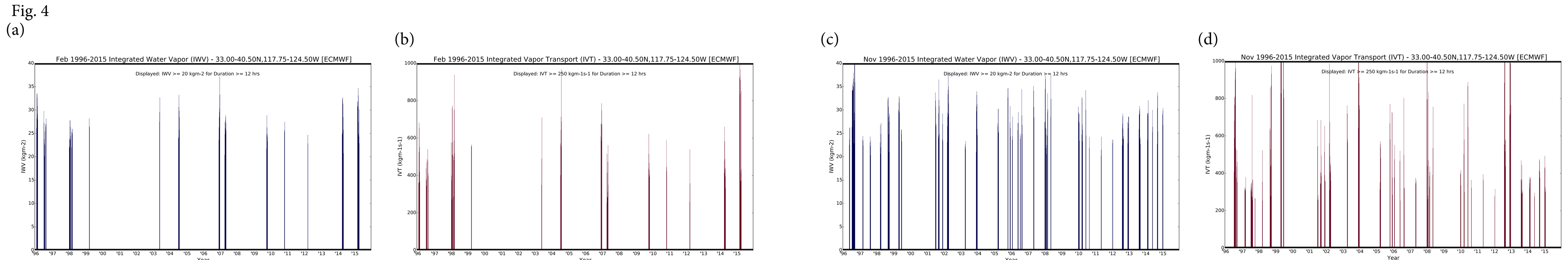

Similar to the single-point analysis, Fig. 4 shows that there are more recorded AR events in November than in February. With the multi-point analysis, a few more ARs that were not present above are present here. For example, the February 2003 AR event is now present in both Fig. 4 (a) and (b), and the November 2003 event is present in both Fig. 4 (c) and (d). Although some ARs, such as the first event of November 1996, are still not captured in both the IWV and IVT plots, there is greater agreement between AR events identified in this study and those in SSM/I-based studies [Dettinger et al. 2011; Neiman et al. 2008 (Met.)] if the analysis is expanded to include multiple points along the coast. It is also worth noting that the durations as well as the peaks of AR events can be slightly greater in Fig. 4 than Fig. 3.

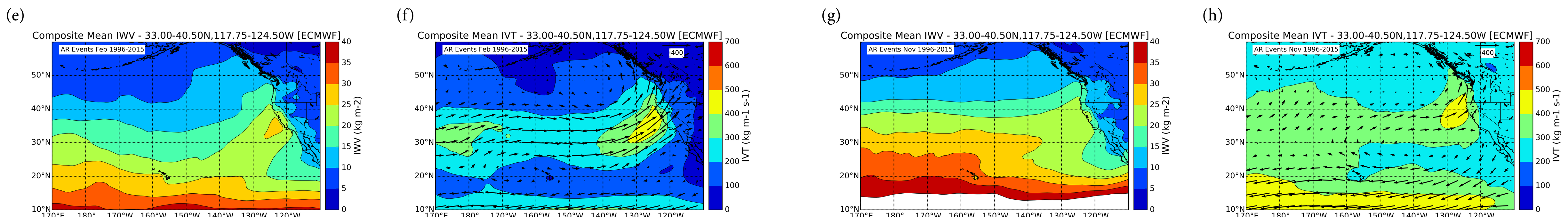

These composite mean IWV and IVT plots portray similar composite ARs—particularly for February—to those in Fig. 3 but generally have a lower maximum value at the core (with the exception of Fig. 4 (e)). The composite mean IVT for November in Fig. 4 (h) shows a more pronounced composite AR compared to Fig. 3 (h), while the structure of Fig. 4 (f), the February composite, appears nearly identical to Fig. 3 (f) when disregarding the lower values at its core.

APPLICATIONS

Machine Learning: Opportunities & Challenges

Traditional methods of detecting ARs in large climate datasets can be tedious and may involve human subjectivity. Instead, "teaching" a machine how to identify these events can yield faster results and potentially reduce bias. A recent study has explored machine learning for this purpose [Liu et al. 2016]. However, the diversity among ARs can be difficult to discern—both for humans and computers. It follows that perhaps a more complete definition of AR events can permit machine learning to be a suitable alternative to current methods of AR identification.

Fig. 5 shows examples based on the February and November datasets that may be used as part of a training set for a neural network to identify ARs in climate datasets. The training set, model, and scripts are a work in progress. Row (a) shows examples of AR events that may be relatively straightforward to identify and (b) shows examples of structures that are not classified as AR events. Row (c), however, illustrates the need to converge on a more fine-tuned definition of AR events and their types: for instance, what constitutes an AR making landfall on the California coast, or an AR in general.

Fig. 5

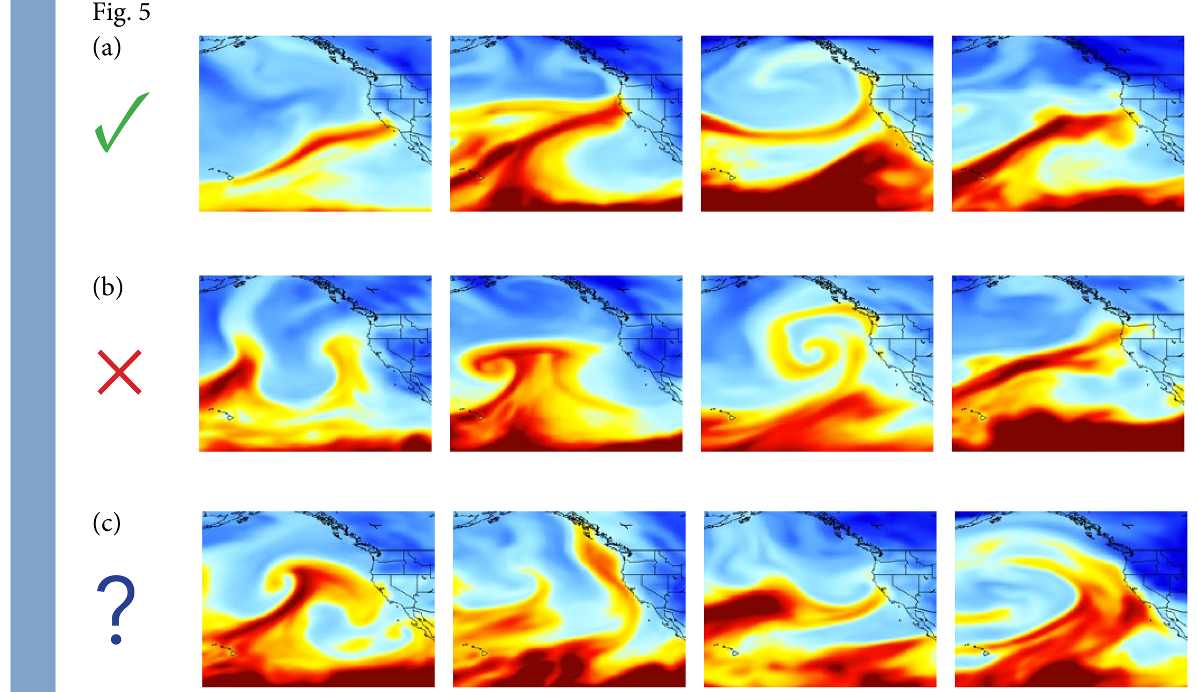

CONCLUSIONS

A previous study focused on characterizing the AR event in early February 2014 and considered this event in a climatological context of recorded ARs occurring in the month of February over the 20-year period from 1996-2015. This study extends the previous analysis with a climatological characterization for the month of November over the same twenty-year period for both single and multiple landfall points along the California coast. There are many more AR events in November (43) across the twenty-year period than in February (15). Additionally, several AR events that are identified in IWV charts are not in IVT charts, or vice versa. With the multiple-point analysis, some of these discrepancies appear to be resolved. Composite means were also calculated. At the core of both the February and November composite ARs, peak IWV of 25-30 mm and peak IVT of 500-600 $kgm^{-1}s^{-1}$ are observed. IWV for the November events extends beyond its core to the tropical water vapor reservoir, which appears at a higher latitude than the February composite. IVT values for the November composite are higher than those of February but form a less-pronounced composite AR. The February composite AR tends to have a more meridional form compared to the November composite AR, possibly linked with the apparent poleward extension of moisture from the tropical water vapor reservoir. The multiple-point analysis shows similar results. However, the composite ARs generally have a lower maximum value at the core and the composite mean IVT for November is more pronounced. The overarching challenge of AR event identification using machine learning techniques is also explored and emphasizes the need to converge on a more fine-tuned definition of ARs. Regional characterizations such as this study can assist in gaining a better understanding of the formation of ARs, their probable trajectories, and impact at landfall. Our ability to forecast these extreme phenomena is crucial for water resource management, flood planning, agriculture, and the economy. Future work for this study includes further development of the algorithms to identify and characterize ARs in climate datasets.

REFERENCES

Dettinger, M. D., F. M. Ralph, T. Das, P. J. Neiman, and D. R. Cayan, 2011: Atmospheric rivers, floods and the water resources of California. *Water 3*, no. 2: 445-478.

Lavers, D. A., G. Villarini, 2013. The nexus between atmospheric rivers and extreme precipitation across Europe. Geophys. Res. Lett. 40, 3259–3264. doi: 10.1002/grl.50636

Liu, Y., E. Racah, Prabhat, J. Correa, A. Khosrowshahi, D. A. Lavers, K. Kunkel, M. Wehner, and W. Collins, 2016: Application of Deep Convolutional Neural Networks for Detecting Extreme Weather in Climate Datasets. *arXiv*, arXiv:1605.01156.

Neiman, Paul J., F. M. Ralph, G. A. Wick, Y. Kuo, T. Wee, Z. Ma, G. H. Taylor, and M. D. Dettinger, 2008: Diagnosis of an intense atmospheric river impacting the pacific northwest: Storm summary and offshore vertical structure observed with COSMIC satellite retrievals. *Mon. Weather Rev.*, 136(11), 4398–4420.

Neiman, Paul J., F. M. Ralph, G. A. Wick, J. D. Lundquist, and M. D. Dettinger, 2008: Meteorological Characteristics and Overland Precipitation Impacts of Atmospheric Rivers Affecting the West Coast of North America Based on Eight Years of SSM/I Satellite Observations. *J. Hydrometeor.*, 9, 22–47.

Ralph, F. M., P. J. Neiman, and G. A. Wick, 2004: Satellite and CALJET aircraft observations of atmospheric rivers over the eastern North Pacific Ocean during the winter of 1997/98. *Mon.Wea. Rev.*, 132(7), 1721-1745.

Ralph, F. M., P. J. Neiman, and R. Rotunno, 2005: Dropsonde observations in low-level jets over the northeastern Pacific Ocean from CALJET-1998 and PACJET-2001: Mean vertical-profile and atmospheric-river characteristics. *Mon. Wea. Rev.*, 133(4), 889-910.

Rutz, J. J., W. J. Steenburgh, and F. M. Ralph, 2014: Climatological characteristics of atmospheric rivers and their inland penetration over the western United States. *Mon. Wea. Rev.*, 142(2), 905921.

Rutz, J. J., W. J. Steenburgh, and F. M. Ralph, 2015: The inland penetration of atmospheric rivers over western north america: A lagrangian analysis. *Mon. Wea. Rev.*, 143(5), 1924-1944.

Zhu, Y. and R. E. Newell, 1998: A proposed algorithm for moisture fluxes from atmospheric rivers. *Mon. Wea. Rev.*, 126(3), 725–735.

(Selected references shown.)

ACKNOWLEDGMENTS

The author of this study gratefully acknowledges the guidance provided by Dr. Paul Ullrich, Assistant Professor of Regional Climate Modeling, Dept. of Land, Air and Water Resources, UC Davis. Many thanks to Dr. Robert B. Schmunk (NASA Goddard) for providing a special beta version of Panoply.